

Thulium-doped optical fibers for fiber lasers operating at around 2 μm

I. KASIK*, M. KAMRADEK, J. AUBRECHT, P. PETERKA, O. PODRAZKY, J. CAJZL,
J. MRAZEK, and P. HONZATKO

¹ Institute of Photonics and Electronics, Czech Academy of Sciences, 57 Chaberska St., Prague 8, 182 51, Czech Republic

Abstract. The paper deals with spectral and lasing characteristics of thulium-doped optical fibers fabricated by means of two doping techniques, i.e. via a conventional solution-doping method and via a nanoparticle-doping method. The difference in fabrication was the application of a suspension of aluminum oxide nanoparticles of defined size instead of a conventional chloride-containing solution. Samples of thulium-doped silica fibers having nearly identical chemical composition and waveguiding properties were fabricated. The sample fabricated by means of the nanoparticle-doping method exhibited longer lifetime, reflecting other observations and the trend already observed with the fibers doped with erbium and aluminum nanoparticles. The fiber fabricated by means of the nanoparticle-doping method exhibited a lower lasing threshold (by $\sim 20\%$) and higher slope efficiency (by $\sim 5\%$ rel.). All these observed differences are not extensive and deserve more in-depth research; they may imply a positive influence of the nanoparticle approach on properties of rare-earth-doped fibers for fiber lasers.

Key words: optical fiber, fiber laser, thulium, aluminum oxide, nanoparticles, solution doping, nanoparticle doping.

1. Introduction

Fiber lasers constitute one of the most spectacular achievements of modern science and engineering. They are frequently used both in applications requiring delicate operation, including medicine and metrology, as well as in high-power applications, such as metal machining, splicing and welding. Following the seminal demonstration of a fiber laser based on neodymium-doped glass fiber [1], and later after the successful demonstration of fiber amplifiers based on erbium-doped silica optical fiber [2–3], there have been a number of developments in the field. High-power fiber lasers have been typically based on erbium- or ytterbium-doped silica fibers [4], and recently, also on thulium-doped silica fibers operating in the 2 μm “eye-safe” spectral region. Thulium fiber lasers are intensively investigated for a wide range of applications in medicine, defense, wireless communications, spectroscopy and material processing [5–11]. Laser physicists have conducted intensive research, achieving development in many aspects of fiber lasers, including flexibility of operating wavelength, growth of laser efficiency, increase of output power, and decrease of lasing threshold. Novel “double-clad” fiber structures have been shown to allow significant increases in laser output power [12]. Another approach to increasing the fiber laser output power has been through the use of novel compositions of glass matrices, specifically via increasing the concentration of rare-earth elements (RE) in a silica matrix. Examples of this can be seen in the co-doping of silica fibers with RE dissolving modifiers, including phosphorus pentoxide (in the case of ytterbium-doped fibers [13–17])

and aluminum oxide [18–19]. The doping of fiber cores with both nanoparticles and RE has been proposed to enhance laser efficiency [20–22]. There have been several comprehensive surveys on this topic [23–24].

In this paper, we study spectral and lasing characteristics of thulium-doped optical fibers fabricated (a) via a conventional solution-doping method, and (b) via a nanoparticle-doping method. This study does not aim at achieving maximum output power of a thulium fiber laser but at evaluation of potential influence of the nanoparticle-doping fabrication method developed on fiber and laser properties.

2. Experimental

2.1. Preform and fiber fabrication. Thulium-doped optical fibers were drawn from preforms fabricated by the modified chemical vapor deposition (MCVD) method [25], and then extended with either the conventional solution-doping method (SD) [26], or a developed “nanoparticle-doping” method (NP) [20–21]. We used a 500 mm long F300 silica substrate tube with 18 mm outer diameter and 1.4 mm wall thickness (Heraeus). We first deposited several buffer layers of pure SiO_2 as optical cladding, after which we deposited a thin porous core layer of SiO_2 submicron particles along the full length of the substrate tube. The variation of deposition temperature was kept carefully within $\pm 5^\circ\text{C}$. The tube was then halved into two sections, with one half processed via the SD protocol, and the second processed via the NP protocol, in order to compare the properties of fibers prepared by each method in a fair manner. Subsequent drying, sintering and collapsing protocols were similar for both substrates.

In the conventional SD method, the core layer was penetrated by a solution containing both aluminum chloride and RE ions. Specifically, we used ethanolic solutions (ethanol absolute,

*e-mail: kasik@ufe.cz

99.9%, VWR) containing thulium (III) chloride hexahydrate ($\text{TmCl}_3 \cdot 6\text{H}_2\text{O}$, 99.99%, Aldrich) of 0.03 mol/l concentration and aluminum chloride (AlCl_3 anhydrous, 99.99%, Aldrich) of 0.3 mol/l concentration. Dipping time was 60 min. The resting liquid was then drained out, the solvent evaporated, and the layer was slowly dried and sintered. Finally, the deposited tube was collapsed into the rod. i.e. the preform.

In the NP method, a suspension of aluminum oxide nanoparticles of <50 nm in size ($\gamma\text{-Al}_2\text{O}_3$, 99.9%, Aldrich) together with thulium (III) chloride hexahydrate ($\text{TmCl}_3 \cdot 6\text{H}_2\text{O}$, 99.99%, Aldrich) was dispersed in ethanol (absolute, 99.9%, VWR). A freshly ultrasonicated suspension was applied in the substrate tube. After penetration of the suspension into the porous layer (counted in seconds), the remaining liquid was drained out and the solvent from the wet layer was evaporated. The suspension was mixed immediately before its application (to avoid potential aggregation of dispersed alumina) and total dipping time was ~ 2 min. The doped layer was slowly sintered into a glassy state and the deposited tube was collapsed into the preform.

The chlorine-containing atmosphere generated by oxidation of gaseous germanium tetrachloride was applied during drying and sintering steps in both our experiments. Preforms were drawn to optical fibers having 125 μm in diameter under the same conditions. An in-house constructed drawing tower was used for the fiber drawing. The tower is equipped with a graphite resistance furnace (Centorr, US), Accuscan 5010 diameter gauges (Beta LaserMike, Belgium), coating die (Sancliff, US), UV curing furnace (Fusion Systems, US), take-up (Heathway, UK) and control system (ID-Lab, CR). We used a drawing temperature of 1950°C and feeding speed of 3.5 mm/min; the delay of the preforms in the hot zone of the furnace was approximately 3 minutes. Fibers were coated with UV-curable DeSolite 3471-3-14 coating during the drawing.

2.2. Preform and optical fiber characterization. Local chemical compositions of the preforms were determined by means of electron microprobe analysis (EPMA) with an integrated scanning electron microscope using a Cameca-SX100 electron probe microanalyzer. The samples were sputtered with a thin

layer of graphite and inspected by a 2 μm beam at an energy of 20 keV. The EPMA limit of detection for the analyzed elements was 0.06 mol% of Al, 0.2 mol% of Ge and 0.1 mol% of Tm.

Refractive-index profiles of the prepared preforms were determined using a A2600 profiler (Photon Kinetics). Profiles were measured at different longitudinal positions and under several angles with a radial resolution of 0.005 mm. Averaged profiles were calculated from individual profiles determined at different angles.

Spectral attenuation of drawn fibers was determined by comparing the transmission properties of the reference and pigtailed tested fibers. A tungsten halogen lamp was used for excitation. Since there is no fiber spectral analyzer operating from 600 to 2100 nm available in our laboratory, spectra were obtained by compilation of data obtained from both an ANDO AQ1425 analyzer (spectral range of 600–1030 nm) and a Nicolet 8700 FTIR spectrometer (spectral range of 1030–2100 nm). Taking account of the dynamic range of these setups, the background losses of the fibers were determined by comparing sections with a length difference counted in hundreds of meters. Absorption bands of OH^- were determined by comparing sections with a length difference counted in meters. The concentration of OH^- was calculated on the basis of attenuation at 1383 nm according to [27]. Absorption bands of thulium ions were determined by measurements of fiber sections with a length counted in centimeters. Concentration of thulium ions was calculated on the basis of absorption peak at 1640 nm and compared to the data obtained by the EPMA. Details of attenuation measurements are given in [19].

2.3. Luminescence and laser characterization. Luminescence lifetime was evaluated from luminescence decay curves recorded by detecting luminescence emitted from the side perpendicular to the stripped optical fiber, i.e. the side detection setup. Details of determination of the lifetimes from single exponential decay curves and lasing characteristics are described in [19].

Laser characteristics were determined using a ring-laser setup shown in Fig. 1. A laser diode emitting at 1570 nm and amplified using EDFA was used for excitation and the output power

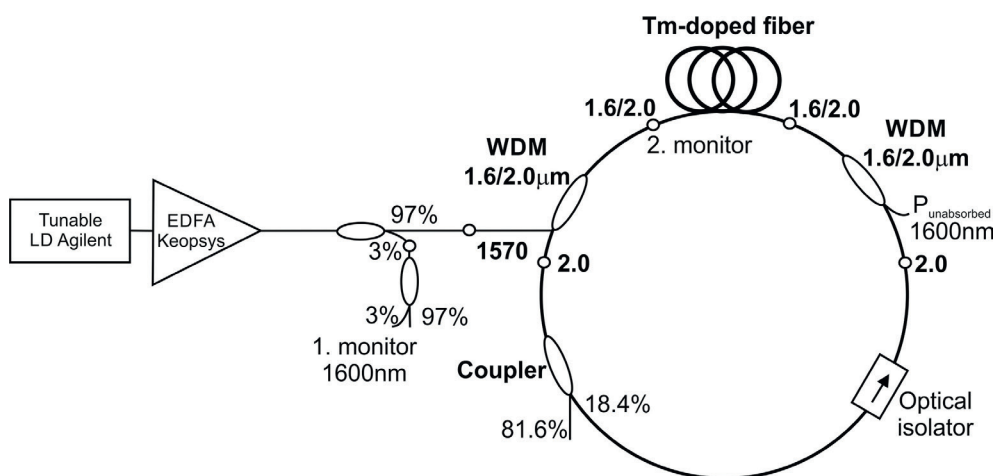


Fig. 1. Ring fiber laser setup used for characterization

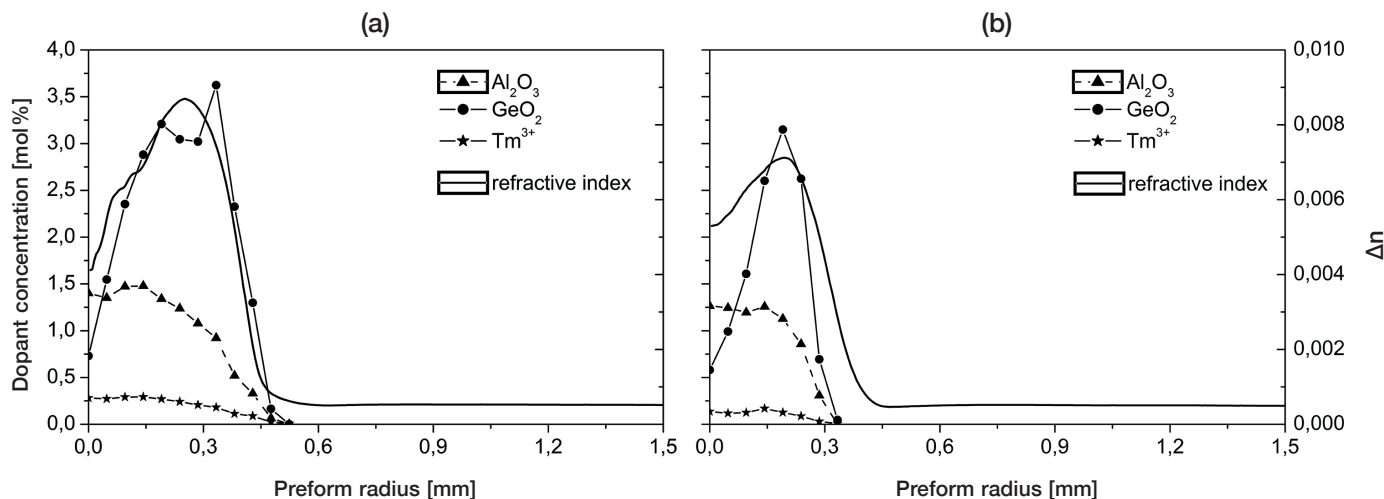


Fig. 2. Refractive-index and concentration profiles of preforms prepared by means of a) the conventional SD method, b) the NP method

of the laser was measured at 1950 nm. Wavelength division multiplexers (WDMs), with branches optimized for 1600 and 2000 nm, were used for launching the input pump and removing the unabsorbed pump radiation from the ring configuration [29]. The real pump power launched into the ring was measured using 1 monitor and then recalculated with respect to the transmission properties of the couplers at 1570 nm. Laser output was measured using ~82% of the output coupler branch, while the remaining radiation was passing in the ring. All splices between fiber components had negligible insertion losses.

3. Results and discussion

3.1. Refractive-index profiles and chemical composition of preforms. We fabricated transparent 9.2 mm diameter preforms without any visible inhomogeneity (phase separation) for fiber drawing. Their refractive-index and concentration profiles can be seen in Fig. 2. The maximum refractive-index difference between the core and the cladding (taken from averaged profiles) was 0.008 in the sample fabricated by means of the conventional SD method and 0.007 in the sample fabricated by means of the NP method. These values correspond to numerical apertures of 0.15 and of 0.14, respectively. The difference between these values was very close, and the mode field diameter of both fibers was also the same (~9.7 μm), thus the cut-off wavelengths calculated according to [28] stood at 1900 nm and 1770 nm, respectively.

The shape of the refractive-index profiles corresponds to the distribution of dopants in each preform; in both preforms, a small drop of refractive index around the central axis can be observed. This corresponds to depletion of germanium dioxide evaporated during preform collapsing [25]. The maximum content of Al₂O₃ was found near the axis of both preforms (with no observed dips near the axis). The distribution of thulium concentration exhibited a similar profile and so a bonding between these two components can be deduced, however, no phase separation in microscopic scale was observed. The

results of the EPMA chemical analyses are summarized in Table 1. As the analyzed values were rounded off according to the limit of detection of the EPMA, it can be concluded that chemical compositions of the fabricated preforms were nearly identical.

Table 1
Chemical composition of preforms determined by the EPMA

sample	Al ₂ O ₃ (max) [mol%]	GeO ₂ (max) [mol%]	Tm ³⁺ (average) [mol%]
SD	1.4	3.1	0.2
NP	1.3	3.4	0.2

3.2. Spectral attenuation of optical fibers. The spectral attenuation of drawn fibers within a range of 550 to 2100 nm can be seen in Fig. 3. Typical absorption bands corresponding to Tm³⁺

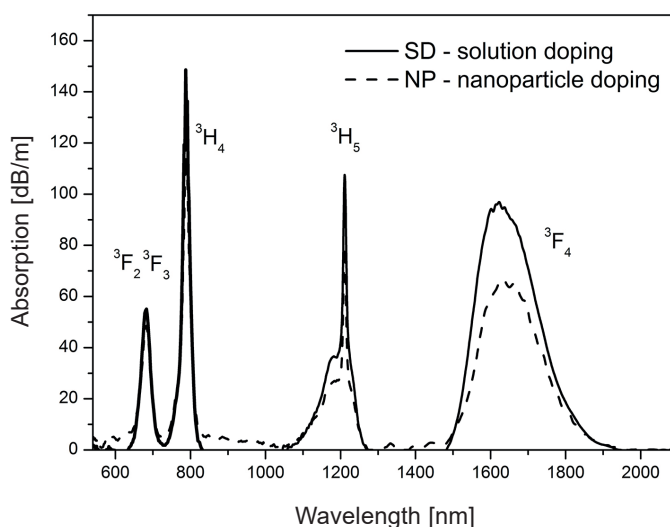


Fig. 3. Spectral attenuation of thulium-doped fibers drawn from preforms fabricated by both the conventional SD method and the NP method

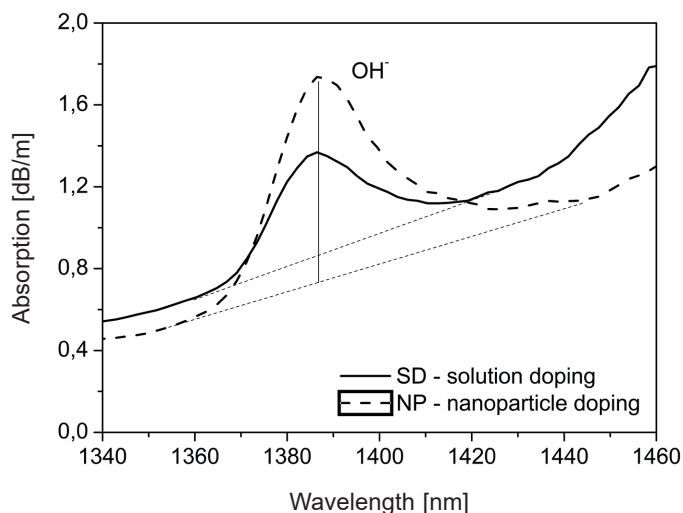


Fig. 4. Attenuation of fibers fabricated by both the conventional SD method and by the NP method in the spectral region corresponding to OH^- absorption

were centered around 682 nm, 787 nm, 1180–1210 nm and 1640 nm. Since the attenuation of fibers was high at these wavelengths, only short fiber sections were characterized (12 cm of fiber fabricated by the SD method, and 14 cm of fiber fabricated by the NP method). It can be seen that absorption bands of the sample fabricated by the NP method are less intense when compared to the sample fabricated by the SD method. Estimated Tm^{3+} concentrations calculated from absorption at 1640 nm were 2500 ppm in the fiber prepared by the SD method, and 1800 ppm in the fiber prepared by the NP method [19]. Taking account of the accuracy of the described method and homogeneity of the samples (typically within 10 rel%), these results reflect the EPMA results (Table 1) to a large extent.

Absorptions of OH^- centered at around 1383 nm (Fig. 4) were of ~ 0.49 dB/m in the fiber fabricated by the SD method (measured length difference of 8 m) and of ~ 0.98 dB/m in the fiber fabricated by the NP method (measured length difference of 4 m). Taking account of the absorption coefficient [27], we calculated an OH^- content of 7 ppm and 14 ppm for the two preforms, respectively.

Hence, the drying process of the porous core layer can be considered to be quite effective and roughly comparable between both fabrication processes. No significant influence of OH^- absorption on minimum background losses at the wavelength of excitation of fiber laser (1570 nm) can be deduced from these results.

Minimum background losses (measured with length difference of 148 m of the fiber fabricated by the NP method and 364 m of the fiber fabricated by the SD method) observed around 550 nm or around 1050 nm were of the same level of ~ 0.03 dB/m.

Cut-off wavelengths calculated at 1900 nm and 1770 nm could not be experimentally determined because they were masked by the tail of the intensive absorption band of Tm^{3+} centered at 1640 nm (Fig. 3).

3.3. Luminescence properties of optical fibers. Fluorescence lifetimes of $^3\text{F}_4$ levels (Fig. 5) were determined to be 430 μs in the fiber prepared by the conventional SD method and 575 μs in the fiber prepared by the NP method. The longer observed lifetime of thulium ions embedded into the fiber core by means of the NP method reflected previous results [19]. The lifetimes of fibers fabricated by the NP method were slightly longer in comparison to those fabricated by the SD method. Since the key parameters influencing the lifetime of thulium ions (Al_2O_3 content in the fiber core and the $\text{Tm}^{3+}/\text{Al}_2\text{O}_3$ ratio) and thermal processing of the fibers were nearly the same, the increase of lifetime of fiber prepared by the NP method can be attributed to a difference of local vicinity of thulium ions in the glass matrix. However, interpretation of the local structure of fiber cores in nanoscale is extremely difficult and exceeds the scope of this paper.

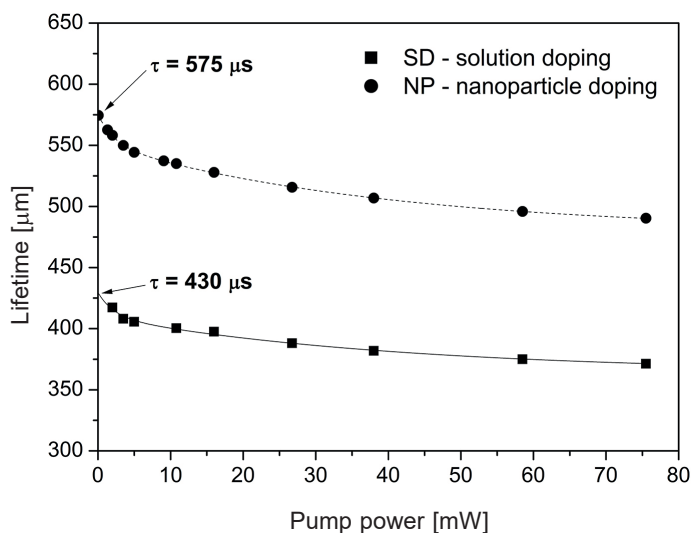


Fig. 5. $^3\text{F}_4$ lifetime of fibers fabricated by the conventional SD method and the NP method

3.4. Lasing characteristics. Fibers prepared via both methods and characterized by Figs. 2–5 were pumped at 1570 nm (Fig. 3). Laser lines shifted with both increasing pump power and active fiber length. The characteristics of each fiber laser having optimized fiber length are shown in Fig. 6. The optimized length of the fiber prepared by the SD method was of 1.16 m and that of the fiber prepared by the NP method was 1.58 m.

Using the same laser setup, lasing thresholds were determined as 405 mW for the fiber prepared by the NP method and 493 mW for the fiber prepared by the conventional SD method. The slope efficiencies (determined using the same laser setup) were 29.8% for the fiber fabricated by the conventional SD method and 31.3% for the fiber fabricated by the NP method. This trend reflected the measured lifetimes of the fibers (Fig. 5) relating to local structure of the glass and partly to homogeneity of the fibers. This trend also reflects the results achieved using fibers doped with erbium aluminum nanoparticles [24], [29–30].

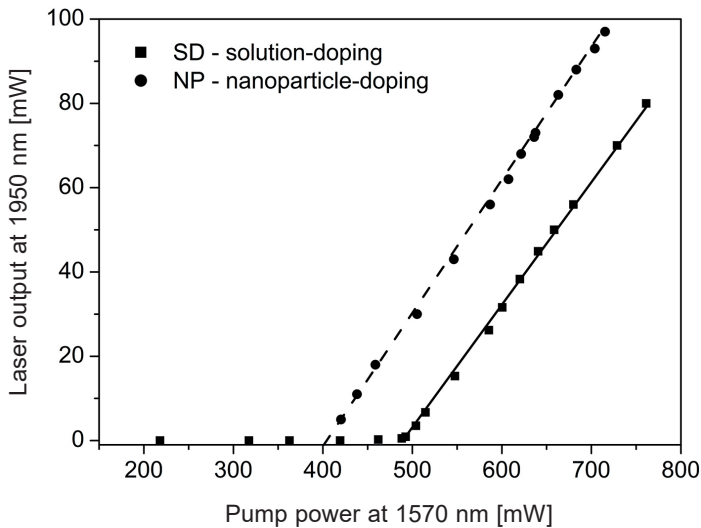


Fig. 6. Ring laser output characteristics measured from fibers fabricated by both the conventional SD method and the NP method

The observed trends in laser threshold and slope efficiency match the theoretical models [31–32]. In the case of a two-level laser system of a fiber laser, both the laser rate and propagation equations can be solved analytically and the formulae for the laser threshold and slope efficiency are known [33]. In such a fiber laser, the threshold depends on the fluorescence lifetime of the upper laser level, but the laser slope does not. Although the thulium-doped fiber laser with multiple energy levels cannot be described by a simple two-level model, the trends should be similar, for example, as was found in the case of thulium-doped fiber lasers [34]. The lower laser threshold of fiber prepared by the NP method can partly be explained also by better homogeneity of the fiber core in micro-scale, described in a general manner in [22].

The slope efficiencies achieved herein were not high when compared to a Fabry-Perot fiber laser setup, where slope efficiencies of about 55% have been routinely achieved; the lower efficiencies measured here are inevitable due to the high number of splices and optical components used in the ring laser. Nevertheless, the laser configuration presented in this paper made it possible to provide proper characterization of doped fibers, as it eliminates a risk of longitudinal mode instability and self-pulsing [27].

4. Conclusions

We have demonstrated spectral and lasing properties of optical fibers doped with Al_2O_3 , GeO_2 and Tm^{3+} fabricated by the conventional SD method as well as the NP method developed herein. When similarly characterized in the same ring laser setup, we observed that the chemical composition and waveguiding properties of these fibers were nearly identical. The sample fabricated by the NP method exhibited longer lifetime, reflecting other observations [19] and the trend already observed with the fibers doped with erbium and aluminum nanoparticles [22]. The fiber fabricated by the described NP method exhib-

ited lower lasing threshold (by $\sim 20\%$) and higher slope efficiency (by $\sim 5\%$ rel.). All these differences observed herein are not extensive and deserve more in-depth research; they may imply a positive influence of the NP approach on properties of RE-doped fibers for fiber lasers. Another study should be feasible because of the robustness of the developed NP technique demonstrated in the similarity of several characteristic properties (when compared to the conventional SD method), including chemical composition, refractive-index profile and cut-off wavelength.

Acknowledgements. This research has been supported by the Czech Science Foundation, project No. 17–20049. Portions of this work were presented at the SPIE Optics + Optoelectronics symposium, 2019. The authors would also like to thank Dr. N. Scott Lynn for his critical reading and correction of English in the manuscript.

REFERENCES

- [1] C.J. Koester and E. Snitzer, “Amplification in a fiber laser”, *Applied Optics* 3, 1182–1186 (1964).
- [2] J.E. Townsend, S.B. Poole, and D. N. Payne, “Solution-doping technique for fabrication of rare-earth-doped optical fibers”, *Electronics Letters* 23(7), 329–331 (1987).
- [3] E. Desurvire, J.R. Simpson, and P. C. Becker, “High-gain erbium-doped travelling-wave fiber amplifier”, *Optics Letters* 12(11), 888–890 (1987).
- [4] D.J. Richardson, J. Nilsson, and W.A. Clarkson, “High power lasers: current status and future perspectives”, *Journal of the Optical Society of America B-Optical Physics* 27, B63–B92 (2010).
- [5] P. Grzes, M. Michalska, and J. Swiderski, “Picosecond mode-locked Tm-doped fibre laser and amplifier system providing over 20 W of average output power at 1994 nm”, *Metrology and Measurement Systems* 25, 649–658 (2018).
- [6] M. Janeczek, J. Swiderski, A. Czernski, B. Zywicka, J. Bujok, M. Szymonowicz, E. Bilewicz, M. Dobrzynski, M. Korczynski, A. Chroszcz, and Z. Rybak, “Preliminary evaluation of thulium doped fiber laser in pig model of liver surgery”, *Biomed Research International*, No. 3275284 (2018).
- [7] A. Sincore, J.D. Bradford, J. Cook, L. Shah, and M.C. Richardson, “High average power thulium-doped silica fiber lasers: Review of systems and concepts”, *IEEE Journal of Selected Topics in Quantum Electronics* 24 (2018), No. 0901808. DOI: 10.1109/JSTQE.2017.2775964
- [8] J. Sotor, G. Sobon, M. Kowalczyk, W. Macherzynski, P. Paletko, and K.M. Abramski, “Ultrafast thulium-doped fiber laser mode locked with black phosphorus”, *Optics Letters* 40, 3885–3888 (2015).
- [9] N.J. Ramirez-Martinez, M. Nunez-Velazquez, A.A. Umnikov, and J.K. Sahu, “Highly efficient thulium-doped high-power laser fibers fabricated by MCVD”, *Optics Express* 27, 196–201 (2019).
- [10] D. Klimentov, N. Tolstik, V.V. Dvoyrin, R. Richter, and I.T. Sorokina, “Flat-top supercontinuum and tunable femtosecond fiber laser sources at 1.9–2.5 μm ”, *Journal of Lightwave Technology* 34, 4847–4855 (2016). DOI: 10.1109/JLT.2016.2604039
- [11] S.D. Jackson, “Towards high-power mid-infrared emission from a fiber laser”, *Nature Photonics* 6(7), 423–431 (2012).

- [12] M.N. Zervas and C.A. Codemard, "High power fiber lasers: A review, *IEEE Journal of Selected Topics in Quantum Electronics* 20, 219–241 (2014).
- [13] G.G. Vienne, J.E. Caplen, L. Dong, J.D. Minelly, J. Nilsson, and D.N. Payne, "Fabrication and characterization of Yb³⁺: Er³⁺ phosphosilicate fibers for lasers", *Journal of Lightwave Technology* 16(11), 1990–2000 (1998).
- [14] A.L.G. Carter, S.B. Poole, and M. G. Sceats, "Flash-condensation technique for the fabrication of high-phosphorus-content rare-earth-doped fibers", *Electronics Letters* 28(21), 2009–2011 (1992).
- [15] J.E. Townsend, W. L. Barnes, and K. P. Jedrzejewski, "Yb³⁺ sensitized Er³⁺ doped silica optical fiber with ultrahigh transfer efficiency and gain", *Electronics Letters* 27(21), 1958–1961, (1991).
- [16] J. Kirchhof, S. Unger, A. Schwuchow, S. Jetschke, and B. Knappe, "Dopant interactions in high power laser fibers", Proc. SPIE 5723, Optical components and materials II, 261–272.
- [17] M.M. Bubnov, A.N. Guryanov, and K.V. Zotov, "Optical properties of fibers with aluminophosphosilicate glass cores", *Quantum Electronics* 39, 857–862 (2009).
- [18] A. Dhar, S. Das, H.S. Maiti, and R. Sen, "Fabrication of high aluminum containing rare-earth doped fiber without core-clad interface defects", *Optics Communications* 283, 2344–2349 (2010).
- [19] J. Cajzl, P. Peterka, M. Kowalczyk, J. Tarka, G. Sobon, J. Sotor, J. Aubrecht, P. Honzatko, and I. Kasik, "Thulium-doped silica fibers with enhanced fluorescence lifetime and their application in ultrafast fiber lasers", *Fibers* 6, 66 (2018). DOI:10.3390/fib6030066
- [20] O. Podrazky, I. Kasik, M. Pospisilova, and V. Matejec, "Use of alumina nanoparticles for preparation of erbium-doped fibers", 2007 IEEE LEOS Annual Meeting Conference Proceedings 1–2, 246–247 (2007).
- [21] A. Pastouret, C. Gonnet, C. Collet, O. Cavani, E. Burov, C. Chaneac, A. Carton, and J.P. Jolivet, "Nanoparticle doping process for improved fibre amplifiers and lasers", Proc. SPIE 7195, Fiber lasers VI, Technology, systems and applications, 2009, 71951X-1–71951X-8.
- [22] I. Kasik, O. Podrazky, J. Mrazek, J. Cajzl, J. Aubrecht, J. Probostova, P. Peterka, P. Honzatko, and A. Dhar, "Erbium and Al₂O₃ nanocrystals -doped silica optical fibers", *Bull. Pol. Ac.: Tech.* 62, 641–646 (2014).
- [23] I. Kasik, P. Peterka, J. Mrazek, and P. Honzatko, "Silica optical fibers doped with nanoparticles for fiber lasers and broadband sources", *Current Nanoscience* 12, 277–290 (2016).
- [24] C.C. Baker, E.J. Friebele, Ch.G. Askins, B.A. Marcheschi, J.R. Peele, W. Kim, J. Sanghera, J. Zhang, M. Dubinskii, and Y. Chen, "Nanoparticle doping for high power lasers at eye safer wavelengths", Proc. Laser congress 2016 (ASSL, LSC, LAC), 2016, AM3A.1.
- [25] S.R. Nagel, J.B. Mac Chesney, and K.L. Walker, "An overview of the modified chemical vapor-deposition (MCVD) process and performance", *IEEE Journal of Quantum Electronics* 18(4), 459–476 (1982).
- [26] J.E. Townsend, S.B. Poole, and D.N. Payne, "Solution-doping technique for fabrication of rare-earth-doped optical fibers", *Electronics Letters* 23, 329–331 (1987).
- [27] J. Aubrecht, P. Peterka, P. Koska, O. Podrazky, F. Todorov, P. Honzatko, and I. Kasik, "Self-swept holmium fiber laser near 2100 nm", *Optics Express* 25, 4120–4125 (2017). DOI:org/10.1364/Oe.25.004120
- [28] D. Marcuse, Principles of optical fiber measurement, Academic Press, New York, 1981.
- [29] E.J. Friebele, C.C. Baker, Ch.G. Askins, J.P. Fontana, M.P. Hunt, J. R. Peele, B.A. Marcheschi, E. Oh, W. Kim, J. Sanghera, J. Zhang, R.K. Pattnaik, L.D. Merkle, and M. Dubinskii, "Erbium nanoparticle doped fibers for sufficient, resonantly-pumped Er-doped fiber laser", Proc. SPIE 9344, Fiber lasers XII: Technology, systems and applications, 934412-1–934412-8 (2015).
- [30] C.C. Baker, E.J. Friebele, A.A. Burdett, D.L. Rhonehouse, J. Fontana, W. Kim, S.R. Bowman, L. B. Shaw, J. Sanghera, J. Zhang, R. Pattnaik, M. Dubinski, J. Ballato, C. Kucera, A. Vargas, A. Hemming, N. Simakov, and J. Haub, "Nanoparticle doping for high power fiber lasers at eye-safer wavelengths", *Optics Express* 25(12), 13903-13915 (2017).
- [31] S.D. Jackson and T.A. King, "Theoretical modeling of Tm-doped silica fiber lasers", *Journal of Lightwave Technology* 17(5), 948–956 (1999).
- [32] M. Pisarik, P. Peterka, J. Aubrecht, J. Cajzl, A. Benda, D. Mares, F. Todorov, O. Podrazky, P. Honzatko, and I. Kasik, "Thulium-doped fibre broadband source for spectral region near 2 micrometers", *Opto-Electronics Review* 24, 223–231 (2016). DOI:10.1515/oere-2016-0022.
- [33] J. Chen, X. Zhu, and W. Sibbett, "Rate-equation studies of erbium-doped fiber lasers with common pump and laser energy bands", *Journal of Optical Society B* 9(10), 1876–1882 (1992).
- [34] P. Peterka, I. Kasik, A. Dhar, B. Dussardier, and W. Blanc, "Theoretical modeling of fiber laser at 810 nm based on thulium-doped silica fibers with enhanced 3H₄ level lifetime", *Optics Express*, 19, 2773–2781 (2011). DOI.org/10.1364/oe.19.002773.